Communications on Applied Nonlinear Analysis
ISSN: 1074-133X
Vol 32 No. 8s (2025)

Influence of Masonry Strength and Column Reinforcement on the Lateral Performance of Infilled RC Frames

Jonathan T Mark[1], Yamini Sreevalli I[2*]

[1]Research Scholar, School of Civil Engineering, Vellore Institute of Technology, Chennai – 600127, India

[2]Associate Professor, School of Civil Engineering, Vellore Institute of Technology, Chennai – 600127, India

[*]Email: yaminisreevalli.i@vit.ac.in

Article History:

Received: *07-11-2024*

Revised: *17-12-2024*

Accepted: *04-01-2025*

Abstract:

Masonry infill strength and column flexural, shear reinforcement are the influencing factors in the lateral performance of infilled frame. Various numerical and experimental studies performed in the past decades bring out the beneficial and adverse effects of masonry infilled frame. In this numerically study masonry of different strengths i.e., Concrete Masonry Unit (CMU), Clay Brick (CB), Flyash brick (FA) and Aerated Autoclaved Concrete block (AAC) have been used as infill in a reinforced concrete frame and the behaviour is observed. Similarly, for strong masonry, CMU infilled frame, the flexural and shear reinforcement of column has been varied. From the numerical analysis performed it has been observed that irrespective of the masonry strength all the specimens showed predominant flexural failure of column whereas CMU infilled frame with a flexural reinforcement of 6.4% failed by shear. It is concluded that when the shear capacity of the frame is more than the flexural shear capacity of the frame the failure mode is observed to be flexure. From the conclusions a simple and effective analytical method for the identification of shear failure in column considering the influence of masonry strength has been proposed.

Keywords: Failure Pattern, Flexural shear capacity, Infill frame, Masonry strength, Shear capacity.

1. INTRODUCTION

The effect of masonry infill on the behavior of Reinforced Concrete (RC) frames subjected to lateral loading has been experimentally and numerically studied by many researchers over the past decades. Both detrimental (Mehrabi et. al., 2003, Basha et. al., 2016) and beneficial (Al Louzi et. al., 2015, Smith et. al., 1967, Calvi et. al., 2001) effects of the influence of masonry on the structure have been reported. The behaviour of RC infilled frames were experimentally by considering various parameters like design of the RC frame, strength of bricks, aspect ratio, vertical loading on columns and beam, type of horizontal loading and number of bays (Mehrabi et. al., 1996). The main outcome of this study was the classification of failure patterns that could occur in a RC frame infilled with masonry wall, subjected to lateral loading. Murthy et. al. (2000) conducted experimental investigations to study the behaviour of twelve single bay single storey RC frames infilled with masonry wall. The specimens were half scaled and were tested under cyclic loading. The parameters varied were the reinforcement and the brick size. From the experiments it was concluded that the presence of infills increased the dissipation capacity when compared to bare RC frames. It was also observed that the masonry infills walls increased the stiffness of the infilled RC frames thereby reducing the deflection. Experimental study was carried out by Colangelo (2005) on the behaviour of thirteen single storey, single bay specimens. The parameter considered was change in design of the frame of specimens. The test frames included both ductile and non-ductile design criteria. It was concluded that the stiffness of the infilled specimens were greater than the stiffness of the bare frame. It can be concluded from these

experimental studies that masonry infill is beneficial in increasing the stiffness of a RC frame under lateral loading and also alters the failure mode of RC frame.

Investigations on the behaviour of half-scaled RC infilled frames were conducted both experimentally and numerically by Al-Charr et. al. (2002). The parameters considered were masonry strength and number of bays. It was observed that masonry infill increased the lateral stiffness of the specimens in comparison with the bare frame specimens. Experiments were conducted by Kakletsis et. al. (2008) on seven single bay, single storey specimens which were scaled to one-third of the prototype. The variation in masonry strength and openings in masonry infills were considered as parameters for this study. It was concluded that contribution of infills in energy dissipation was greater when compared to contribution to strength. Experimentally study on the behaviour of single bay, single bay RC frames infilled with different types of masonry was performed by Zovkic et. al. (2013). Irrespective of the strength of the infill, there was an increase in the stiffness due to the masonry infill. Experiments were performed on four full-scaled single storey, single bay specimens by Huang et. al. (2016). Three types of masonry namely solid clay bricks, hollow clay bricks and aerated concrete blocks were used for the experiment. It was concluded that the infilled frames performed better than the bare frame in terms of strength and stiffness and also the performance of all specimens were discussed concluding that the specimen with hollow clay bricks suffered severe damage during testing. The failure patterns of the specimens at different stages of drift were given. The behaviour of five half scale single storey, single bay specimens were experimentally studied by Alwashali et. al. (2019) in which the parameters considered were the mortar strength and Beta Index (ratio of strength of frame to infill). The specimen with higher Beta index had better seismic capacity. Experimentally investigations on two full-scale masonry infilled RC frames under cyclic loading were carried out by Wararuksajja et. al. (2020). A design strategy has been proposed for local failure elimination in frames due to the resistance of the masonry infills.

Numerically investigations were performed to study the effect of masonry infills on RC frames (2017). Large parametric studies of the previous experimental investigations were collected and a simplified relation was proposed with relative stiffness and relative strength of infill to frame. The proposed relation can be used to predict and avoid shear failure of columns in structures. A review study was conducted on various modelling approaches like micro, meso and macro modelling for capturing the non-linear behaviour of masonry (Nasiri et. al., 2017, Hak et. al., 2012, Nicola et. al. 2015). It was concluded that macro modelling techniques were not effective in capturing the frame-infill interactions though it has the advantage of simplicity in design and computation. Numerical studies were conducted on behaviour of many RC infilled frames with varying parameters of infills and horizontal loading using finite element modelling by Mohamed et. al. (2018). It was concluded that finite element modelling can be adopted to capture the non-linear behaviour of masonry infilled RC frames, can be used as an alternative to the experimental investigation of physical specimens. Numerical study on twenty-three specimens from various experimental investigations using ABAQUS software was conducted by Al Louzi et. al. (2018). In order to identify the failure of masonry infilled RC frames, the parameters relative strength and relative stiffness of the specimens were used to propose a simple methodology. To define the shear and flexure failure patterns in specimens, a new hysteric model was developed.

From the above literature review, it was perceived that many experimental investigations have studied the beneficial effect of masonry infill and how it alters the failure of RC frames. Few notable works only suggested the shear failure in columns due to the presence of masonry infills. In this work an attempt has been made to study the failure mode of column by varying masonry infill strength, column flexural and shear reinforcement.

2. DETAILS OF THE SPECIMENS

The masonry infilled RC frame specimens for study were adopted from Mehrabi et. al. (1996). The specimens were designed in accordance with ACI 318-19. Half-scaled specimens with dimension of 60.5 in x 90 in (1500 mm x 2250 mm) were used in the study. The concrete used in the frames had a compressive strength of 4.5 ksi (30.9 MPa). The yield strength of longitudinal bars was 60 ksi (413.4 MPa). The yield strength of stirrups was 53 ksi (365 MPa). RC frame rests on a solid foundation with dimension 18 in x 18 in x 122 in. A displacement controlled load of 2 inch was applied from the left side on the vertical face of beam**.** The concrete material considered for this study had a density of 2.23 E-06 kip / in^3, elastic modulus of 3180 ksi and poisson's ratio of 0.2. The steel reinforcement considered for this study had a density of 7.236 E-06 kip / in^3, elastic modulus of 29000 ksi and poisson's ratio of 0.3.

In the first parametric study the stirrup spacing in the columns and beams were 2.5 in throughout the members with all other dimensions and properties of RC frame being the same. Four types of masonry were used in this study as infill namely Concrete Masonry Unit (CMU), Clay Brick (CB), Flyash bricks (FA) and Aerated Autoclaved Concrete blocks (AAC). The properties of CMU were adopted from [6]. The properties of CB and FA were adopted from [4]. The properties of AAC blocks were adopted from the author's experimental work. Elastic properties of various types of infill are tabulated in Table 1. Total of five specimens have been considered for analysis in ABAQUS software. The five specimens were Bare Frame (BF), frame with CMU (FI CMU), frame with CB (FI CB), frame with FA (FI FA) and frame with AAC (FI AAC).

In the second parametric study the detailing of the columns alone has been changed. Concrete Masonry Unit adopted from [6] was selected as the masonry for all the specimens. In the first specimen (FI CMU S5) stirrups spacing was increased to 5 in from 2.5 in while maintaining the same percentage of longitudinal reinforcement (3.2 %) as in FI CMU. In the second specimen (FI CMU S5 L6.4) the stirrup spacing was increased to 5 in and the percentage of longitudinal reinforcement was increased to 6.4 %. In the third specimen (FI CMU S5 L6.4 AL) vertical load of 33 kips (146 kN) were applied on top of each column of FI CMU S5 L6.4. The dimensions and detailing of specimens considered in both parametric study are shown in Figure-1.

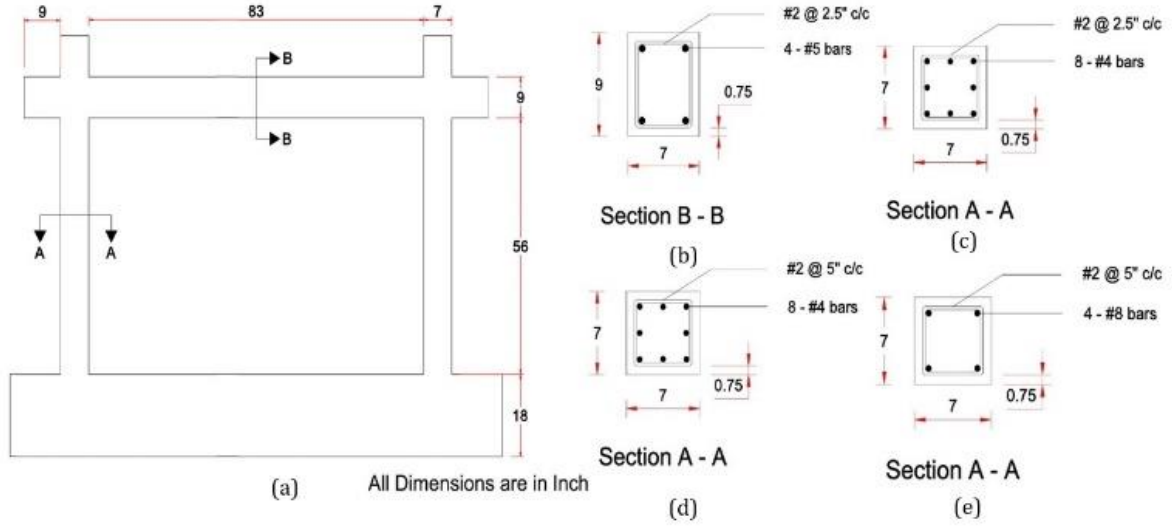

Figure 1 - (a) Dimensions of the RC Frame **(b)** Detailing of the Beam section **(c)** Detailing of Column section of first parametric study **(d)** Detailing of Column section of FI CMU S5 **(e)**Detailing of Column section of FI CMU S5 6.4 and FI CMU S5 6.4 AL

Table 1 Properties of Masonry Infill

Masonry	Density (kip/in^3)	Modulus of Elasticity (ksi)	Poisson ratio
CMU	2.155 E-06	1965	0.2
CB	5.7 E-05	333.81	0.2
FA	5.52 E-05	211.46	0.2
AAC	7.5 E-05	73.3	0.2

3. FINITE ELEMENT MODELLING VALIDATION

Bare frame and the infilled frame specimen 2 of Mehrabi et. al., has been modelled and analysed in ABAQUS 6.23. Maximum load attained and load displacement behaviour of the specimens is considered for validation. Material plasticity model, meshing of structural elements, boundary conditions and interface, play a key role in simulating and validating the behavior of the experimental specimen. Modelling parameters considered in the study are as follows:

3.1 Material Model

The material models are used to input the elastic and plastic properties of concrete, steel and masonry in Abaqus. Some of the material model that are available in Abaqus library, which are used to simulate the non-linear behavior are Druker Prager, Concrete Smeared cracking and Concrete Damage Plasticity (CDP). In this study CDP has been chosen to define the material properties where the plasticity, compressive behaviour and tensile behaviour are given as input. The plasticity property for this model is adopted from Nasiri et. al. (2017). The plastic property of the model is determined by parameters namely dilation angle, eccentricity, the ratio of biaxial to uniaxial compressive yield (fb_0/fc_0), K and viscosity parameter. The CDP parameters are given in Table-2. The compressive and tensile behaviour of the masonry and concrete are defined using yield stress, cracking strain and damage parameter values. Damage parameter for different materials is defined for the erosion of elements.

Table-2. Plasticity parameters of CDP model

Dilation Angle	Eccentricity	fb0/fc0	K	Viscosity Parameter
18	0.1	1.16	0.667	0.001

3.2 Interface

In the model the interface has been defined between the frame concrete and the masonry and also within the bricks of masonry. The masonry brick in this model has been defined as a brick surrounded by half mortar. Interactions were assigned between the inner surface of RC frame and mortar layers using ‘surface to surface’ interaction conditions. The interaction property was defined using three parameters namely ‘Cohesive behavior, Tangential behavior and Damge’. The conditions for node interaction and separation parameters were defined in Cohesive behavior. For tangential behaviour a friction coefficient of 0.87 was assigned. The evolution, stabilization and initiation of damage, which defines the traction behavior were given as input in the Damage parameter (Al Louzi et. al., 2015). The interaction was defined as master and slave as given in the software. The reinforcement and the concrete in the frame were constrained by ‘embedded region’ property available in the software. This property binds the reinforcement within the frame concrete as in the physical specimen. The modelling of the bricks and interface has been shown in Figure-2.

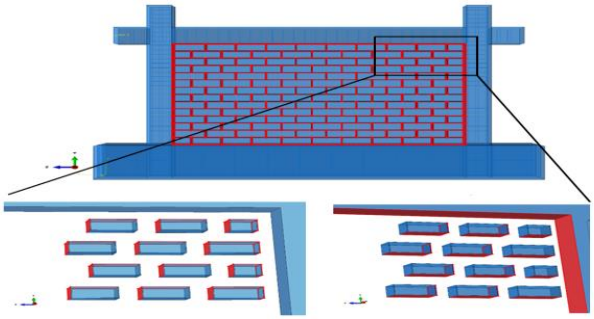

Figure 2 - Master surface (Right) and Slave surface (left) of the specimens [Adapted from Mark et. al. (2021)]

3.3 Meshing

Meshing the specimens plays an important role in determining the accuracy of the results. Hence mesh sensitivity analysis was conducted to determine the suitable mesh size. Mesh size of 1 in, 1.5 in, 2 in and 2.5 in were considered and the simulation results were compared with specimen 1 (Bare Frame of Mehrabi et. al.) respectively. Table-3 represents the mesh sensitivity analysis of the bare frame. The mesh size of 1.5 in and 2.5 in had less error percentage in comparison with 2 in and 1 in mesh size in terms of maximum lateral load of the specimens. The computational time of analysis of specimen with 1.5 in mesh size was much more than the specimen with 2.5 in mesh size. Hence 2.5 in mesh size was adopted for the specimens of this study.

Table-3. Analysis of mesh sensitivity for bare frame specimen

Mesh Size (in)	No. of Elements	Maximum Load (kips)			Error (%)	Computational Time (hours)
		Mehrabi's		Numerical		
		Experimental	Numerical			
2.5	9,422	23.88	27.50	26.91	-2	4
2	13,474			32.2	17	6
1.5	21,386			26.8	-2	11
1	50,243			20.96	-23	103

The infilled frames were also subjected to mesh sensitivity analysis which were compared with the experimental results of specimen 2 (Infilled frame of Mehrabi et. al.). Mesh size of 1.5 in, 2 in and 2.5 in were considered for the study, the results of which have been presented in Table-4. The specimens with mesh size of 2 in performed better than specimens with 2.5 in and 1.5 in mesh size, in terms of maximum lateral load of the specimen. Taking the computational time into consideration, the mesh size of 2.5 in was considered for this numerical study.

Table-4. Mesh Sensitivity Analysis of Infilled Frame

Mesh Size (in)	No. of Elements	Maximum Load (kips)		Error (%)	Computational Time (hours)	Initial Stiffness (kips / in)
		Experimental (Mehrabi)	Numerical			
2.5	29,655	33.85	37.61	11	48	117.33
2	33,974		35.93	6.1	168	91.43
1.5	60,578		44.68	32	192	131.2

Failure of the specimen was considered based on the yielding of stirrups (53 ksi) or the yielding of longitudinal bars (60 ksi) whichever occurs first. Shear failure or flexural failure of the specimen was determined based on the yielding of stirrups or longitudinal bars respectively.

The failure patterns at yielding of longitudinal bars have been compared and also the load vs displacement graph of the experimental and numerical specimen has been presented in Figure 3 and Figure 4. The failure of specimen - 2 of Mehrabi was mentioned as the yielding of longitudinal bars at 0.7 inch displacement. The failure of the numerical specimen was also due to the yielding of longitudinal bars but at 0.9 inch displacement. From the graph shown in Figure 4 it can seen that the maximum load carrying capacity of the experimental specimen was 32 kips while the maximum load carrying capacity of the numerical specimen was 37 kips.

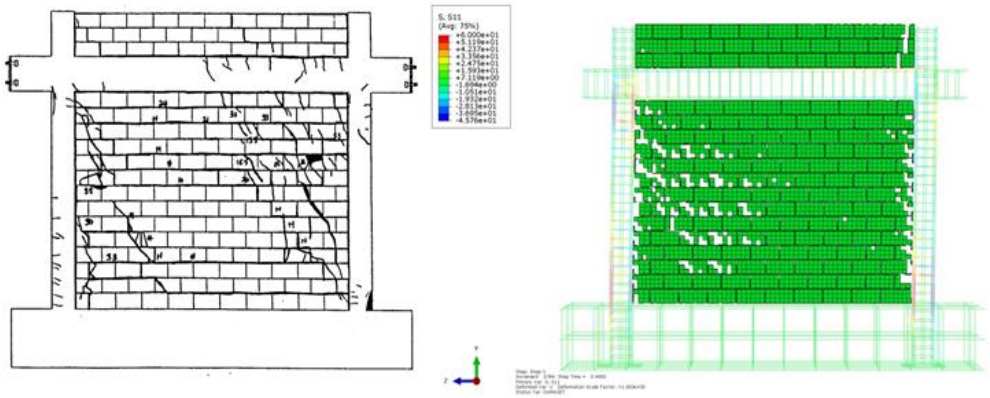

Figure 3 - Comparison of crack pattern at yielding of flexural reinforcement

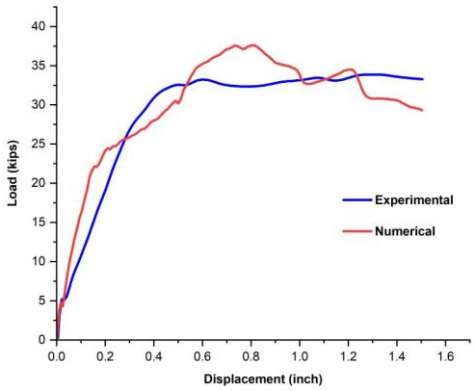

Figure 4 - Comparison of Load displacement curve of Mehrabi and Numerical simulation

4 RESULTS AND DISCUSSION

Numerical analysis has been carried out on all the eight specimens. All the models were modelled with a mesh size of 2.5 in. The failure pattern (tensile damage), yielding of reinforcement, load at yielding of reinforcement and maximum load attained by the specimen have been noted. Tensile damage distribution is considered to represent the failure pattern of specimens as mentioned by many of the researchers in the literature. The distribution of tensile damage of all the specimens at yield of flexural reinforcement and the reinforcement stress has been summarized from Figure-5 to Figure-14.

4.1 First Parametric Study

Figure 5 shows the tensile damage distribution and axial stress distribution of bare frame (BF) at 0.8 in displacement. It can be observed that the longitudinal reinforcement in the columns near the foundation has reached the value of 60 ksi and started yielding which denotes flexural failure. The specimen attained a maximum load of 15.55 kips at 1.04 in displacement.

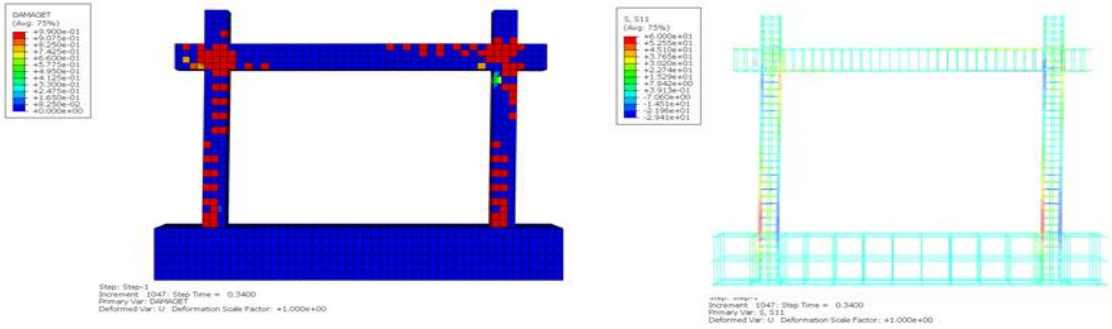

Figure 5 - (left) Distribution of Tensile Damage and **(right)** Reinforcement stress of BF at 0.8 in displacement

In FI CMU specimen initial crack in the column was observed at 25 kips whereas a crack observed in masonry at 38 kips. Cracks in masonry were unevenly distributed and sliding at the mortar joints is noted. Longitudinal bars yielded at a displacement of 0.74 in (44.48 kips) and stirrup in the leeward column near foundation reached yield stress as shown in Figure 6. With further increase in load the longitudinal reinforcement in the windward column completely yielded and the specimen attained a maximum load of 46.03 kips at 1.15 in.

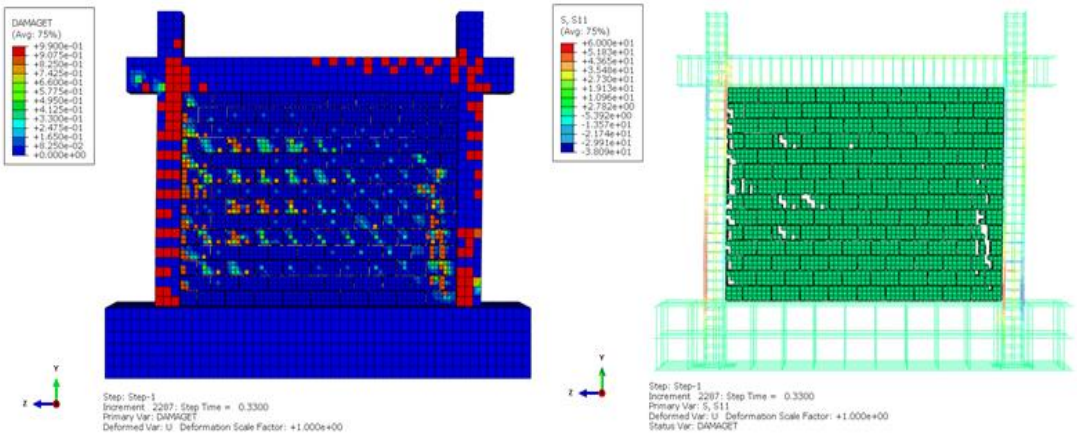

Figure 6 - (left) Distribution of Tensile Damage and **(right)** Reinforcement Stress of FI CMU at 0.74 in displacement

In FI CB specimen initial crack in masonry was observed at 10 kips, with further increase in load at 11 kips distribution of cracks in masonry were spread and appeared as major diagonal crack. Figure 7 shows the longitudinal reinforcement yield of FI CB specimen at a displacement of 0.63 in (23.78 kips). Yielding of stirrups has not been observed even in further steps of analysis. The specimen attained a maximum load of 25.81 kips at 0.96 in displacement.

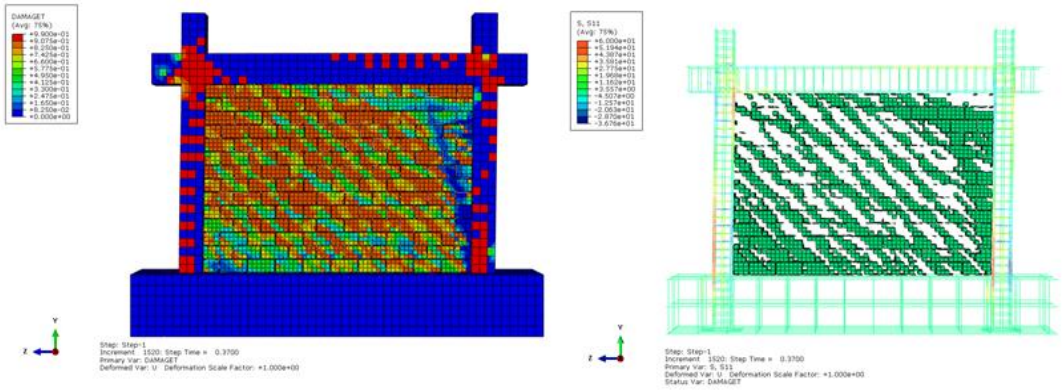

Figure 7 - (left) Distribution of Tensile Damage and **(right)** Reinforcement Stress of FI CB 0.63 in displacement

An initial crack in FA masonry observed at 9 kips and further increase showed a major diagonal crack at 11 kips. Longitudinal reinforcement yielded at a displacement of 0.72 in (24.59 kips) in FI FA specimen as shown in Figure 8. The specimen attained a maximum load of 27.57 kips at 1.5 in displacement. Flexural cracks in columns were observed.

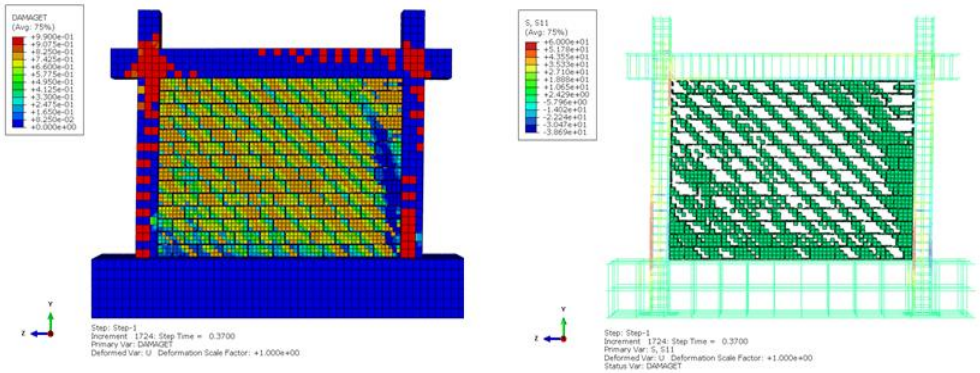

Figure - 8 (left) Distribution of Tensile Damage and **(right)** Reinforcement Stress of FI FA at 0.72 in displacement

In FI AAC specimen also cracks were observed initially in masonry at 7 kips and major diagonal crack at 9 kips. Yielding of longitudinal reinforcement at a displacement of 0.85 in (22.19 kips) is observed and shown in Figure 9. The specimen attained a maximum load of 22.62 at 1 in displacement.

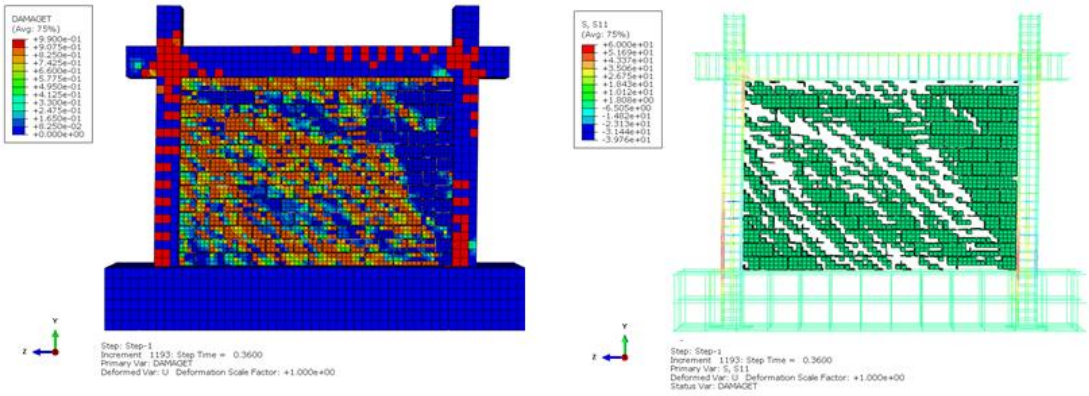

Figure 9 - (left) Distribution of Tensile Damage and **(right)** Reinforcement Stress of FI AAC at 0.85 in displacement

It can be seen that in all the specimens yielding of longitudinal reinforcement was observed followed by flexural cracks in columns. Yielding of stirrups even at a higher displacement is not observed in the specimens. Even though in specimen with strong masonry, FI CMU, few stirrups yielded in the leeward column cracks did not progress in the column. To understand further the possibility of shear failure in FI CMU specimen three specimens were considered for further analysis.

4.2 Second Parametric Study

In FI CMU S5 specimen the yield of longitudinal reinforcement was observed at a displacement of 0.72 in (41.31 kips) as shown in Figure 10. No noticeable yielding of shear stirrups has been observed. The specimen attained a maximum load of 43.58 kips at a displacement of 0.57 in whereas FI CMU attained maximum load at a displacement of 1.15 in, which shows that spacing of stirrups helps in attaining a ductile behavior of the specimen.

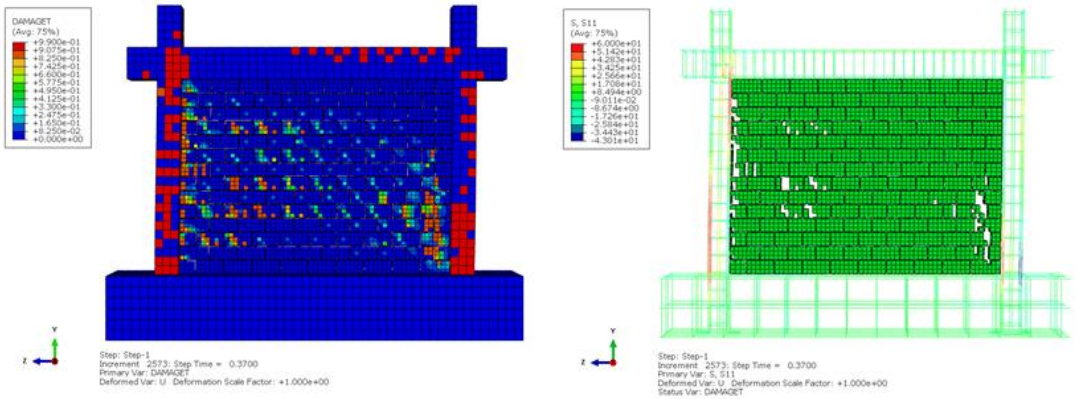

Figure 10 - (left) Distribution of Tensile Damage and **(right)** Reinforcement Stress of FI CMU S5 0.72 in displacement

In FI CMU S5 L6.4 specimen the initial cracks in the masonry were observed followed by the yielding of stirrup at a displacement of 0.6 in (50.1 kips) at the top corner of the windward column and near the foundation in the leeward column, instead of initiation of yield in longitudinal reinforcement as shown in Figure 11. The specimen attained a maximum load of 51.92 kips at 0.7 in displacement. The final failure of the specimen noted a captive column effect, signifying shear failure as shown in Figure 12.

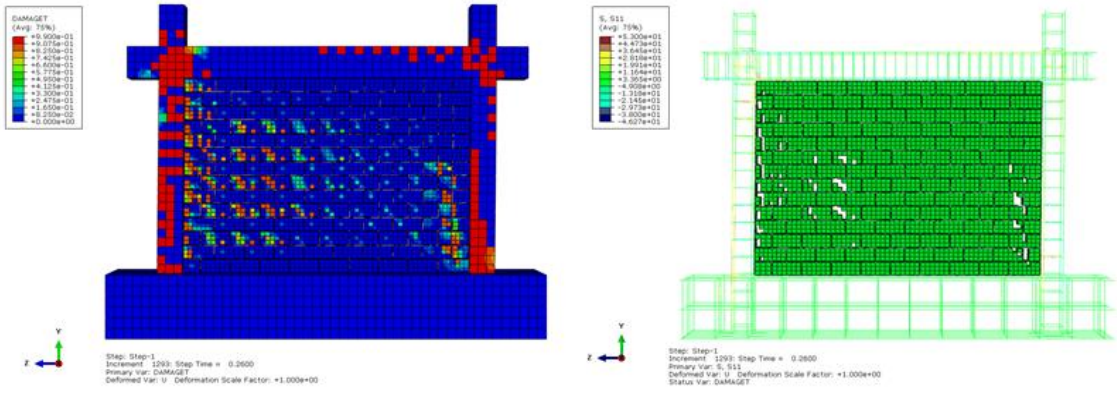

Figure 11 - (left) Distribution of Tensile Damage and **(right)** Reinforcement Stress reinforcement of FI CMU S5L6.4 at 0.6 in displacement

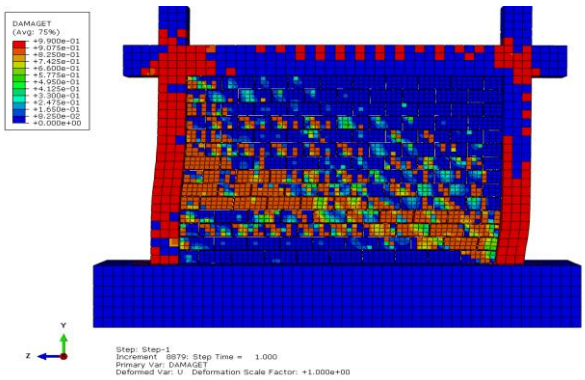

Figure 12 - Tensile damage distribution in FI CMU S5 L6.4 at failure

In FI CMU S5 L6.4 AL specimen, 33 kips axial load is applied at the top of both the columns. Here too the stirrup yielded at a displacement of 0.5 in (56.34 kips) before the longitudinal reinforcement yielded as shown in Figure 13. The specimen had a maximum load bearing capacity of 56.37 kips at 0.44 in displacement. It can be noted that the load carrying capacity has increased compared to FI CMU S5 L6.4 due to the presence of axial load. The final failure in the column which signifies a shear failure is shown in Figure 14.

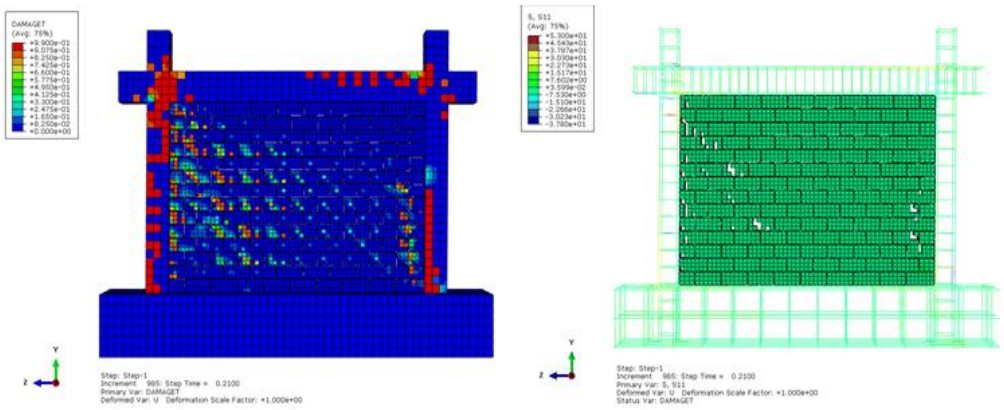

Figure - 13 (left) Distribution of Tensile Damage and **(right)** Reinforcement Stress of FI CMU S5 L6.4 AL at 0.5 in displacement

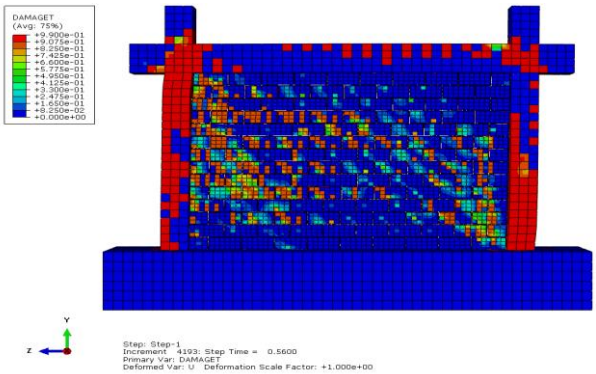

Figure 14 - Tensile damage distribution in FI CMU S5 L6.4 AL at failure

The load vs displacement graphs for the specimens has been shown in Figure 15 and Figure 16. It can be seen that the specimen FI CMU is capable of taking maximum load when compared to other specimens. When compared to the bare frame the load carrying capacity of FI CMU is 66.22 % higher. The initial stiffness of the specimen with FI CMU was 173 kip / in which was much higher than the

other specimens. The initial stiffness of the bare frame specimen was calculated as 31.42 kip / in. The initial stiffness of the specimen with FI CMU was 81 % higher than that of the bare frame specimen. Other specimens FI CB, FI FA and FI AAC exhibited nearly the same initial stiffness of 63.81 kips / in, 51.38 kips / in and 60.96 kips / in respectively.

The initial stiffness of FI CMU S5, FI CMU S5 L6.4 and FI CMU S5 L6.4 AL was observed to be same. Specimens with longitudinal reinforcement 6.4% showed a sudden drop drown in load carrying capacity after attaining the maximum load.

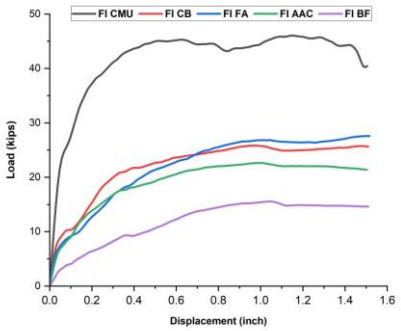

Figure 15 - Load vs Drift relation for the specimens with varying infill strength

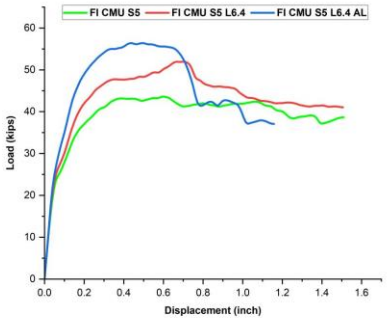

Figure 16 - Load vs Drift relation for the specimens with shear stirrup spacing of 5 in

It can be observed from the above numerical results that only specimens FI CMU S5 L6.4 and FI CMU S5 L6.4 AL failed by shear which has been initiated by the yielding of stirrups. The reason for this being, the shear capacity of the specimen is less than the flexural shear capacity, leading to the failure of specimens by shear which is discussed in detail below.

5. PROPOSED METHOD FOR SHEAR PREDICTION IN COLUMNS

The main aim for which this numerical study has been conducted is to propose a methodology to predict the nature of failure of columns, whether due to flexure or shear. For this puropose a new index named as the S_{col} index (Shear index for columns) has been proposed in this study. The S_{col} index can be defined as the ratio of shear capacity of the column to the flexural capacity of the column with respect to the shear demand imposed on the column due to the presence of masonry infill. The S_{col} index considered includes the participation of the both infill and frame. The index parameters are explained as follows.

$$S_{col} = \frac{V_{f,flex}}{V_{f,sh}}$$

The flexural capacity of the column was calculated from the sectional analysis of the column.

$$V_{f,flex} = 4 * \frac{M_p}{H}$$

Where,

M_p is the ultimate moment carrying capacity of the column in the frame

H is the height of the frame

The shear capacity of the column was calculated to be the sum of shear capacities of concrete and the stirrups. The shear capacity of the specimens was given as per ACI 318-19.

$$V_{f,sh} = 2 * (V_s + V_c)$$

Where,

V_s is the shear capacity provided by the stirrups,

$$V_s = \frac{0.8 * f_{yv} * A_{sv} * d}{s}$$

V_c is the shear capacity provided by the concrete,

$$V_c = \frac{2 * \sqrt{(f_c * 1000)} * b_c * h_c}{1000}$$

f_{yv}, A_{sv} and s represent the yield strength of the stirrup, cross sectional area of the stirrup and spacing of the stirrups respectively. d represents the effective depth of the column. f_c, b_c and h_c represent the compressive strength of the concrete, breadth of the column cross-section, depth of the column cross-section respectively.

The equation for the shear demand due to the masonry infill on the column, V_{infill} has been adopted form FEMA 306 considering diagonal compression failure in masonry infill.

$V_{infill} = W_{ef} * t_{inf} * f_m * Cos\,\theta$

Where,

$W_{ef} = 0.175 * (\lambda_h * H)^{-(0.4 * d_m)}$

$\lambda_h = \sqrt[4]{\frac{E_w * t_w * Sin(2\theta)}{4 * E_c * I_c * h}}$

λ_h is the equation for relative stiffness of the masonry infill to the column, proposed by Smith (1961).

From Table-5 it can be seen that the specimens of the first parametric study have the same values of $V_{f,\,sh}$ and the $V_{f,\,flex}$ as the specimens have the same dimensions and detailing of the RC frame. The specimens of second parametric study differ from the flexural and shear capacity of the first parametric study due to the change in percentage of longitudinal reinforcement and the spacing of shear stirrups. It can be observed that when the flexural capacity was less than the shear capacity the specimens failed by flexure even when the spacing of the stirrups were increased from 2.5in c/c to 5in c/c. When the percentage of longitudinal reinforcement was increased to 6.4 % the flexural shear capacity was more than the shear capacity which led to failure of the specimens by shear. This can be explained in terms of the proposed method for prediction of shear failure in columns, i.e., when the S_{col} of the specimens was less than 1, the failure of the specimens was found to be flexural failure and when S_{col} of the specimens was more than 1, the failure of the specimens was found to be shear failure.

It can also be observed that even when the shear demand due to the presence of infill in FI CMU specimens is more than the shear capacity of the column, the failure of the specimens were determined by the flexural and shear capacities of the columns which is given by the shear prediction method. These observations led to the conclusion that the presence of masonry infill increased the strength and stiffness of the specimens but did not have influence on the failure of columns irrespective of the strength of the masonry infill. Further investigations have to be carried out experimentally in order to verify the conclusions observed from this numerical study.

Table-5. Flexural shear capacity and shear capacity of specimens

Specimen		V_{infill}	$V_{f,sh}$	$V_{f,flex}$	Shear Index, S_{col}	Failure Mode
First Parametric Study	FI CMU	43.57	29.44	15.80	0.54	Flexure

	FI CB	20.35				Flexure
	FI FA	15.80				Flexure
	FI AAC	20.14				Flexure
Second parametric Study	FI CMU S5	43.57	19.81	15.80	0.8	Flexure
	FI CMU S5 L 6.4	44.07	19.81	25.58	1.29	Shear
	FI CMU S5 L6.4 AL	44.07				Shear

6. CONCLUSION

Numerical investigations have been carried out in eight single-bay, single-storey specimens with variation in type of masonry and percentage of reinforcement. The study focusses on the influence of masonry and column reinforcement percentage on the failure mode of columns in a masonry infilled RC frame structure. Analytical investigation based on the equations were carried out and methodology for prediction of shear failure in columns has been proposed. It was observed that when the S_{col} index is less than 1 the failure was observed as flexural failure in the columns of the specimens. When the S_{col} index was more than 1 the failure was observed to be shear failure in the columns of the specimens. It can be seen that even though the type of masonry was varied in the specimens, the failure mode was affected only by the variation in longitudinal and shear reinforcement. This simplified method can be easily and effectively used for prediction of shear failure in columns in a masonry infilled RC frame. It was evident from the study that the presence of masonry increased the strength and stiffness of the specimens but does not have much influence over the failure mode. The percentage of longitudinal and transverse reinforcement in columns influences the failure mode of the columns. The conclusions from the study have been presented here.

- All the specimens of the first parametric study failed predominantly by flexure which was indicated by the yielding of longitudinal reinforcement.
- The initial stiffness of FI CMU was 81% higher than that of the bare frame. The load carrying capacity of this specimen was 66.22% higher when compared to the bare frame.
- Higher the elastic modulus of the masonry, higher was the initial stiffness of the specimens.
- The specimen FI CMU has performed better by yielding in flexure at higher load and less drift percentage when compared to the other specimens
- The initial stiffness attained by the specimens BF, FI CMU, FI CB, FI FA and FI AAC were 31.42 kips/in, 173 kips/in, 63.81 kips/in, 51.38 kips/in and 60.96 kips/in respectively.
- The specimens FI CMU S5 L6.4 and FI CMU S5 L6.4 AL were observed to have a captive column effect leading to shear failure.
- A simple and effective analytical method for the prediction of shear failure in column considering the shear demand from the masonry infill has been proposed.

CONFLICT OF INTEREST

The authors declare that there are no conflicts of interest regarding the publication of this manuscript.

AUTHOR CONTRIBUTION STATEMENT

Author 1: Developed the theory and performed the computations.

Author 2: Proposed the research problem, verified the analytical methods and supervised the findings of this work.

REFERENCES

[1] A. B. Meharbi, P. B. Shing, "Seismic analysis of masonry-infilled reinforced concrete frames," TMS Journal, vol. 21, no. 1, pp. 81-94, 2003.

[2] S. H. Basha, H. B. Kaushik, "Behavior and failure mechanisms of masonry-infilled RC frames (in low-rise buildings) subject to lateral loading," Eng. Struct, vol. 111, pp. 233-45, 2016, https://doi.org/10.1016/j.engstruct.2015.12.034.

[3] Al Louzi, "Seismic in-plane response of reinforced concrete frames with masonry infill walls," Ph.D. Dissertation, Purdue University, West Lafayette, Indiana, 2015.

[4] B. S. Smith, "Methods for predicting the lateral stiffness and strength of multi-storey infilled frames," Building Science, vol.2, no. 3, pp. 247-57, 1967, https://doi.org/10.1016/0007-3628(67)90027-8.

[5] G. M. Calvi, D. Bolognini, "Seismic response of reinforced concrete frames infilled with weakly reinforced masonry panels," J. Earthq. Eng., vol. 02, pp. 153-85,2001, https://doi.org/10.1080/13632460109350390.

[6] A. B. Mehrabi AB, P. B. Shing, M. P. Schuller, J. L. Noland, "Experimental evaluation of masonry-infilled RC frames," J. Struct. Eng., vol. 122, no.3, pp. 228-37, 1996, https://doi.org/10.1061/(ASCE)0733-9445(1996)122:3(228).

[7] C. V. R. Murthy, S. K. Jain, "Beneficial influence of masonry infill walls on seismic performance of RC frame buildings," in 12th World conference On Earthquake Engineering, Auckland, New Zealand, January, 2000.

[8] F. Colangelo, "Pseudo-dynamic seismic response of reinforced concrete frames infilled with non-structural brick masonry," Earthquake engineering & structural dynamics, vol. 34, no.10, pp. 1219-1241, 2005, https://doi.org/10.1002/eqe.477.

[9] G. Al-Chaar, M. Issa, S. Sweeney, "Behavior of masonry-infilled nonductile reinforced concrete frames,"J. Struct. Eng., vol. 128, no. 8, pp. 1055-1063, 2002, https://doi.org/10.1061/(ASCE)0733-9445(2002)128:8(1055).

[10] D. J. Kakaletsis, C.G. Karayannis, "Influence of masonry strength and openings on infilled R/C frames under cycling loading," J. Earthq. Eng., vol. 12, no. 2, pp. 197-221, 2008, https://doi.org/10.1080/13632460701299138.

[11] J. Zovkic, V. Sigmund, I. Guljas, "Cyclic testing of a single bay reinforced concrete frames with various types of masonry infill," Earthq. Eng. Struct. D., vol. 42, no. 8, pp. 1131-1149, 2013, https://doi.org/10.1002/eqe.2263.

[12] Q. Huang, Z. Guo, J. S. Kuang, "Designing infilled reinforced concrete frames with the 'strong frame-weak infill'principle," Eng. Struct., vol. 123, pp. 341-353, 2016, https://doi.org/10.1016/j.engstruct.2016.05.024.

[13] H. Alwashali, D. Sen, K. Jin, M. Maeda, "Experimental investigation of influences of several parameters on seismic capacity of masonry infilled reinforced concrete frame," Eng. Struct., vol. 189, pp. 11-24, 2019, https://doi.org/10.1016/j.engstruct.2019.03.020.

[14] W. Wararuksajja, J. Srechai, S. Leelataviwat, "Seismic design of RC moment-resisting frames with concrete block infill walls considering local infill-frame interactions," Bull. Earthq. Eng., vol. 18, pp. 6445-6474, 2020, https://doi.org/10.1007/s10518-020-00942-9.

[15] J. M. Tempestti, A. Stavridis, "Simplified method to assess lateral resistance of infilled reinforced concrete frames," 16th World Conference in Earthquake Engineering, Santiago, Chile, January, 2017.

[16] E. Nasiri, Y. Liu, "Development of a detailed 3D FE model for analysis of the in-plane behaviour of masonry infilled concrete frames," Eng. Struct., vol. 143, pp. 603-16, 2017, https://doi.org/10.1016/j.engstruct.2017.04.049.

[17] S. Hak, P. Morandi, G. Magenes, T. J. Sullivan, "Damage control for clay masonry infills in the design of RC frame structures," J. Earthq. Eng., vol. 16, no. sup1, pp. 1-35, 2012, https://doi.org/10.1080/13632469.2012.670575.

[18] T. Nicola, C. Leandro, C. Guido, S. Enrico, "Masonry infilled frame structures: state-of-the-art review of numerical modelling," Earthq. Struct., vol. 8, no. 3, pp. 733-759, 2015, https://doi.org/10.12989/eas.2015.8.1.225.

[19] H. M. Mohamed, X. Romao, "Performance analysis of a detailed FE modelling strategy to simulate the behaviour of masonry-infilled RC frames under cyclic loading," Earthq. Struct., vol. 14, no. 6, pp. 551-565, 2018, https://doi.org/10.12989/eas.2018.14.6.551.

[20] R. Allouzi, A. Irfanoglu, "Development of new nonlinear dynamic response model of reinforced concrete frames with infill walls," Adv. Struct. Eng., vol. 21, no. 14, pp. 2154-2168, 2018, https://doi.org/10.1177/1369433218768915.

[21] Building code requirements for structural concrete (ACI 318-19): An ACI Standard; Commentary on building code requirements for structural concrete, 2019.

[22] J. T. Mark, I. Y. Sreevalli, "Numerical study on lateral performance of RC frame with strong masonry infill. Asian J Civ Eng, vol. 22, pp. 551–563, 2021. https://doi.org/10.1007/s42107-020-00331-2

[23] Gurusamy.V, Anbarasu, M. Vijayakumar, Y.K., AIP Conference Proceedings, Behaviour of concrete-encased steel Castellated beam: A review , 2023, 2782, 020163

[24] Gopalakrishnan, R., Mohan, A., Sankar, L. P., & Vijayan, D. S. (2020). Characterisation On Toughness Property Of Self-Compacting Fibre Reinforced Concrete. In Journal of Environmental Protection and Ecology (Vol. 21, Issue 6, pp. 2153–2163).

[25] Mohan, A., Tabish Hayat, M.: Characterization of mechanical properties by preferential supplant of cement with GGBS and silica fume in concrete, Materials Today: Proceedings, 2020, 43, pp. 1179–1189.

[26] Dharmar, S., Gopalakrishnan, R., Mohan, A.: Environmental effect of de nitrification of structural glass by coating TiO2, Materials Today: Proceedings, 2020, 45, pp. 6454–6458.

[27] Prabha, G., Dinesh Kumar, R.,Alteration for fine aggregate of concrete with the use of m-sand and low density polypropylene plastic waste as sustainable solution, Journal of Green Engineering, 2020, 10(5), pp. 2291–2303

[28] V.Saravana Karthika, A.Mohan, R.Dinesh Kumar and Chippymol James, Sustainable Consideration by Characterization of Concrete through Partial Replacement of Fine Aggregate Using Granite Powder and Iron Powder, Journal of Green Engineering, Volume-9, Issue-4, December 2019, 514-525.

[29] Mohan A, Saravana Karthika, Ajith J, Lenin dhal, "Investigation on Ultra-High Strength Slurry Infiltrated Multiscale Fibre Reinforced Concrete" Materials Today: Proceedings 22(2020) 904-911.

[30] Mohan, A., Prabha, G. and V., A. 2023. Multi Sensor System and Automatic Shutters for Bridge- An Approach. International Journal of Intelligent Systems and Applications in Engineering. 11, 4s (Feb. 2023), 278–281.

[31] Prabha , G. , Mohan, A. , Kumar, R.D. and Velrajkumar, G. 2023. Computational Analogies of Polyvinyl Alcohol Fibres Processed Intellgent Systems with Ferrocement Slabs. International Journal of Intelligent Systems and Applications in Engineering. 11, 4s (Feb. 2023), 313–321.

[32] Mohan, A., & K, S. . (2023). Computational Technologies in Geopolymer Concrete by Partial Replacement of C&D Waste. International Journal of Intelligent Systems and Applications in Engineering, 11(4s), 282–292.

[33] Mohan, A., Dinesh Kumar, R. and J., S. 2023. Simulation for Modified Bitumen Incorporated with Crumb Rubber Waste for Flexible Pavement. International Journal of Intelligent Systems and Applications in Engineering. 11, 4s (Feb. 2023), 56–60.